SIS epidemics coupled with evolutionary social distancing dynamics

Keith Paarporn and Ceyhun Eksin

Abstract—A major factor contributing to the difficulties in epidemic forecasting is the unpredictable nature of the population behavior that can either mitigate or exacerbate the spread of a disease. In this paper, we consider a game-theoretic framework for modeling the disease prevalence dependent response of the population behavior in a susceptible-infected-susceptible (SIS) epidemiological model. Our behavioral response model is based on replicator dynamics, where the individuals' underlying payoffs dynamically change in response to the prevalence of the disease. The coupled dynamics highlight the interplay between the epidemic state and distancing behaviors. We establish a critical threshold on the incentive parameters for which below the threshold, the state in which the disease is endemic and the population does not cooperate with the recommended public health measures is globally asymptotically stable (GAS). Above the threshold, we find through extensive numerical simulations that a variety of dynamical outcomes emerge. For some parameters, an interior equilibrium in which the endemic state is mitigated and a fraction of the population socially distancing is stable. For other parameters, a stable limit cycle about this interior state emerges. The arising rich set of dynamics demonstrate the potential of the modeling framework for epidemic forecasting.

I. INTRODUCTION

The public's willingness to comply with recommended public health measures, e.g. masking, social distancing, can dramatically alter the trajectory of the disease in a population as evidenced by multiple peaks and varying outbreak sizes across different localities during the COVID-19 pandemic [1], [2]. The mounting evidence on behavior driven trajectory of the COVID-19 pandemic spurred strong interest in modeling of population response during the pandemic [3]-[7]. In such models, behavior of the population evolves endogenously in tandem with disease prevalence. Such mechanistic models of population awareness and behavior during a disease outbreak documented potential issues and biases in disease forecasting when behavior is unaccounted for [8], [9]. These early mechanistic models focused on the mitigating effects of behavior on disease spread. Yet, population behavior not just mitigated but often exacerbated disease spread during the COVID-19 [3], [10]. Moreover, mechanistic models often rely on feedback mechanisms with conceptual parameters that are hard to estimate using data given the complexity of understanding population incentives.

Recently, game-theoretic modeling of population behavior emerged as a more principled approach to modeling popula-

This work is partially supported by NSF ECCS-1953694, NSF CCF-2008855, and CSI Cybersecurity Initiative Senate Bill 18-086. K. Paarporn is with the Department of Computer Science at the University of Colorado, Colorado Springs. C. Eksin is with the Department of Industrial and Systems Engineering at Texas A & M University. Contact: kpaarpor@uccs.edu, eksinc@tamu.edu.

tion behavior [5], [11]–[14]. In a game-theoretic framework, the perceived costs and benefits of public health measures are the explicit and tangible parameters of the behavior model that are easier to estimate [15]. When the costs and benefits are also coupled with the disease dynamics, they exhibit rich set of dynamics including growing oscillations and bifurcations [5], [12], [13], [16], [17].

In this paper, we consider the same game-theoretic framework as the one considered in [13]. In particular, the perceived benefits of the recommended public health measures is dynamically coupled with the disease prevalence. The public's cooperation level evolves according to replicator dynamics taking into account the current cooperation level, where the underlying matrix game payoffs from cooperation and defection changes as the disease prevalence changes. The replicator dynamics drives the public cooperation level toward an equilibrium when the disease state is constant. In our setting, the disease and replicator dynamics evolve in tandem. Specifically, we consider SIS (susceptible-infectedsusceptible) disease dynamics in which the transition rate from S to I is modulated by the cooperation level of the population. We note that the model exhibits a similar set of dynamics as those observed in [13], [17].

In the standard SIS disease dynamics, there are two equilibria: 1) disease-free and 2) endemic equilibria, that are globally stable respectively when the infection rate is less or greater than the healing rate. In our coupled SIS and evolutionary behavior model, we also have the global asymptotic stability (GAS) of the disease-free state (Theorem 3.1), if the infection rate is less than the healing rate— identical to the condition established in [13]. Considering simplified disease dynamics, i.e. the SIS model, allows us to establish payoff conditions for the GAS of the endemic equilibrium under full defection when infection rate is larger than the healing rate (Theorem 4.2). In particular, the payoff condition depends on both the infection and healing rates inherent to the disease, and the relation between the game payoff parameters in disease-free (good) and disease prevalent (bad) states. We also numerically analyze the local stability of endemic equilibrium with partial cooperation levels for payoff parameter values that do not satisfy the payoff conditions for GAS of the endemic equilibrium under full defection. Our simulations identify payoff parameter regions for GAS of the endemic equilibrium under partial cooperation, and stable limit cycles indicating the existence of bifurcations. These results demonstrate that a rich set of dynamics arise as a result of the coupling between game-theoretic behavior and disease dynamics, even for the simplest of disease dynamics.

II. COUPLED SIS EPIDEMIC MODEL

A. SIS epidemic model

We consider a well-mixed population of unit mass. The disease state of an individual is either susceptible or infected. Let $i \in [0,1]$ be the fraction of infected individuals and s=1-i be the fraction of susceptible individuals. In the SIS epidemic model, these evolve according to the following dynamics

$$\dot{i} = \beta \cdot (1 - x) \cdot i \cdot s - \alpha \cdot i
\dot{s} = -\beta \cdot (1 - x) \cdot i \cdot s + \alpha \cdot i$$
(1)

where $\beta>0$ is the rate at which infected individuals transmit the disease to susceptibles, $\alpha>0$ is the rate at which infected individuals heal from the disease, and $x\in[0,1]$ is the proportion of individuals in the population that comply with recommended health measures, e.g. social distancing. In the next section, we will assume that x changes over time according to an evolutionary game dynamic coupled with the state of the epidemic (1). That is, incentives for individuals to take recommended actions dynamically change as the state of the environment, i.e. the fraction of infected individuals i, changes.

B. Evolutionary social distancing dynamics

In the framework of feedback-evolving games [18], we consider individuals in a population that either *cooperate* with recommended health measures, or *defect* from them. The incentives to either cooperate or defect is determined by an environmental state – here, we will take the susceptible fraction s as the environmental state. We say the environment is good if s=1, and bad if s=0. Individuals evaluate payoffs by comparing their current strategy to other strategies in the population according to the payoff matrix

$$A_s = s \begin{bmatrix} R_1 & S_1 \\ T_1 & P_1 \end{bmatrix} + (1 - s) \begin{bmatrix} R_0 & S_0 \\ T_0 & P_0 \end{bmatrix}$$
 (2)

where the first row corresponds to the payoff of a cooperator against another cooperator (first column) or a defector (second column). Similarly, the second row denotes the payoffs to a defector. In a bad environmental state (s=0), the payoff matrix is given as A_0 . We will not place any restrictions on the structure of A_0 .

In a good environmental state (s=1), we will assume the payoff entries in the matrix A_1 follow a Prisoner's Dilemma game. They satisfy $\delta_{TR1} \triangleq T_1 - R_1 > 0$ and $\delta_{PS1} \triangleq P_1 - S_1 > 0$. Here, defection becomes a dominant strategy. The interpretation of this assumption is that when there is no disease circulating in the population, individuals will have no incentive to follow the recommended public health measures.

Individuals occasionally learn about the strategies of other members in the population and their payoffs, upon which they have an opportunity to revise their strategy¹. Given that a fraction $x \in [0,1]$ of individual are cooperators (and 1-x are defectors) and environmental state $s \in [0,1]$, the average payoff to a cooperator and defector are given, respectively, as

$$u_{\mathcal{C}}(x,s) \triangleq x \cdot R_s + (1-x) \cdot S_s$$

$$u_{\mathcal{D}}(x,s) \triangleq x \cdot T_s + (1-x) \cdot P_s$$
(3)

where R_s , S_s , T_s , and P_s are defined as the entries of (2). We assume the fraction of cooperators x evolves according to the replicator dynamics

$$\dot{x} = x(1-x)(u_{\mathcal{C}}(x,s) - u_{\mathcal{D}}(x,s)).$$
 (4)

The fraction of cooperators increases if the payoff a cooperator attains in the population exceeds the payoff that a defector attains, and decreases otherwise.

Overall, we will focus on the following autonomous dynamical system with state $p = (x, i) \in \Gamma \triangleq [0, 1]^2$:

$$\dot{x} = F_x(x,i) \triangleq x(1-x)(u_{\mathcal{C}}(x,1-i) - u_{\mathcal{D}}(x,1-i))
\dot{i} = F_i(x,i) \triangleq \beta \cdot (1-x) \cdot i \cdot (1-i) - \alpha \cdot i$$
(5)

The above system dynamics admit unique solutions because they are polynomial functions on a compact domain, and are thus locally Lipschitz. Through standard arguments (e.g. Nagumo theorem), the interior of the state space, $\Gamma^o \triangleq (0,1)^2$, is positively invariant with respect to the system (5).

Lemma 2.1. If
$$(x(0), i(0)) \in \Gamma^o$$
, then $(x(t), i(t)) \in \Gamma^o$ for all $t \geq 0$.

We are interested in identifying equilibrium points and conditions for which they are globally asymptotically stable.

Definition 1. An equilibrium point $p^* \in \Gamma$ is globally asymptotically stable (GAS) if for any solution of (5) with initial condition $(x(0), i(0)) \in \Gamma^o$, it holds that $\lim_{t\to\infty} (x(t), i(t)) = p^*$

We consider a point to be GAS if all trajectories starting in the *interior* Γ^o converge to it.

III. RESULTS: DISEASE-FREE EQUILIBRIUM

In this section, we consider the regime $\beta \leq \alpha$ where the infection rate is smaller than the healing rate. We find that the disease-free equilibrium under full defection, $\boldsymbol{p}_{\text{DFE}}=(0,0)$ is globally stable.

Theorem 3.1. Suppose $\beta \leq \alpha$. Then the disease-free equilibrium with full defection, $\mathbf{p}_{DFE} = (0,0)$, is GAS.

Proof. First, we observe that the only equilibrium points of the system (5) that lie in Γ are the isolated points (0,0) and (1,0). One can verify that the point p_{DFE} is locally stable.

¹The process in which agents revise their strategies is called a revision protocol [19]. Many distinct types of revision protocols, e.g. pairwise comparison, induce the replicator dynamics. For agents to perform these revision protocols, it is not necessary for them to physically interact with one another in order to learn about others' payoffs – these may be learned through information sources such as media and social networks. Thus, we assume the interactions that underlie the replicator equation do not factor in to the physical epidemic spreading process.

The point (1,0) is a saddle that attracts only the trajectories starting on the border $\{(x,i): x=1, i\in [0,1]\}$. Moreover, $F_i(x,i)<0$ for all $(x,i)\in\Gamma^o$. Hence, there cannot exist a periodic orbit in Γ^o . By the Poincaré-Bendixson Theorem, the point $p_{\rm DFE}$ must be GAS.

In this scenario, any disease outbreak becomes eradicated and the population ceases to follow any health measures.

IV. RESULTS: ENDEMIC EQUILIBRIUM WITH FULL DEFECTION

In this section, we present our main findings on the stability of equilibrium points of (5) under the regime $\beta>\alpha$ where the infection rate is larger than the healing rate. We find that an endemic equilibrium with full defection, $p_D^*=(0,1-\frac{\alpha}{\beta})$ emerges in this regime. In this equilibrium, the disease is not eradicated, yet the entire population ceases to follow any health measures.

Recall that while we place assumptions on the structure of the payoff matrix A_1 (we will assume that the payoff parameters δ_{TR1} , $\delta_{PS1}>0$ are fixed throughout), we do not place any restrictions on the structure of A_0 , i.e. the payoffs in the bad environmental state. Our results will hence specify conditions on the deviation parameters $\delta_{SP0} \triangleq S_0 - P_0$ and $\delta_{RT0} \triangleq R_0 - T_0$, which measures the payoff advantage (or disadvantage) in the bad environment that $\mathcal C$ has over $\mathcal D$ against a defector and cooperator, respectively. The result below specifies conditions for which p_D^* is asymptotically stable.

Theorem 4.1. Suppose $\beta > \alpha$. Then the endemic equilibrium with full defection, $\mathbf{p}_D^* = (0, 1 - \frac{\alpha}{\beta})$ is locally stable if and only if

$$\delta_{SP0} < \delta_{SP0}^* \triangleq \frac{\alpha}{\beta - \alpha} \delta_{PS1}.$$
 (6)

Proof. The Jacobian of the dynamics at an arbitrary point p to be

$$J(\mathbf{p}) = \begin{bmatrix} \frac{\partial F_x}{\partial x}(x,i) & \frac{\partial F_x}{\partial i}(x,i) \\ -\beta i(1-i) & \beta(1-x)(1-2i) - \alpha \end{bmatrix} \tag{7}$$

where

$$\frac{\partial F_x}{\partial x}(x,i) = x(2-3x) \left[i\delta_{RT0} - (1-i)\delta_{TR1} \right] + (1-x)(1-3x) \left[i\delta_{SP0} - (1-i)\delta_{PS1} \right]$$

$$\frac{\partial F_x}{\partial i}(x,i) = x^2(1-x)(\delta_{RT0} + \delta_{TR1}) + x(1-x)^2(\delta_{SP0} + \delta_{PS1})$$
(8)

At the point p_D^* , the Jacobian is

$$J(\mathbf{p}_{D}^{*}) = \begin{bmatrix} u_{\mathcal{C}}(0, \frac{\alpha}{\beta}) - u_{\mathcal{D}}(0, \frac{\alpha}{\beta}) & 0\\ -\alpha(1 - \frac{\alpha}{\beta}) & \alpha - \beta \end{bmatrix}$$
(9)

The characteristic polynomial becomes

$$(\lambda - (\alpha - \beta)) \cdot (\lambda - \epsilon((1 - \frac{\alpha}{\beta})\delta_{SP0} - \frac{\alpha}{\beta}\delta_{PS1})) = 0 \quad (10)$$

The first eigenvalue $\alpha-\beta$ is negative. The second eigenvalue is negative if and only if $f_D(0,\frac{\alpha}{\beta})>f_C(0,\frac{\alpha}{\beta})$, or equivalently, $(1-\frac{\alpha}{\beta})\delta_{SP0}-\frac{\alpha}{\beta}\delta_{PS1}<0$.

Note that p_D^* is unstable if and only if the opposite condition holds. Viewing $(\delta_{SP0}, \delta_{RT0}) \in \mathbb{R}^2$ as the payoff parameter space, p_D^* is stable in the half-space defined by $\delta_{SP0} < \delta_{SP0}^*$, where δ_{SP0}^* is a constant. We will refer to this region where the payoff advantage of a cooperator over a defector in the bad environment is less than δ_{SP0}^* as the *left half-space*. While Theorem 4.1 asserts that p_D^* is locally stable, we can further establish that it is globally asymptotically stable in a large sub-region of the left half-space.

A. Global asymptotic stability in the left half-space

The following result provides conditions on the parameter space for which global asymptotic stability (GAS) of p_D^* can be established.

Theorem 4.2. The equilibrium p_D^* is GAS if $(\delta_{SP0}, \delta_{RT0})$ belongs to the region

$$\{\delta_{SP0} < \delta_{SP0}^*\} \setminus \left\{\delta_{RT0} \ge \frac{1}{2b_2} \left[-b_1 + \sqrt{b_1^2 - 4b_0b_2} \right] \right\}$$

where

$$b_0 \triangleq (a_0 + \delta_{SP0} + \frac{\alpha}{\beta} \delta_{TR1})^2 - 4\delta_{SP0} a_0$$

$$b_1 \triangleq -2(1 - \frac{\alpha}{\beta})(a_0 + \delta_{SP0} + \frac{\alpha}{\beta} \delta_{TR1}) + 4a_0 \qquad (12)$$

$$b_2 \triangleq (1 - \frac{\alpha}{\beta})^2$$

with
$$a_0 \triangleq (1 - \frac{\alpha}{\beta})(\delta_{SP0} - \delta_{SP0}^*)$$
.

The above result provides sufficient conditions for p_D^* to be GAS. We note that p_D^* appears to be GAS in the omitted region in (11) via extensive numerical simulations² of the state trajectories (Figure 1 Center). In the omitted region, two additional interior equilibrium points emerge.

We now develop the analysis to establish Theorem 4.2. The *i*-isocline is

$$I_{i} \triangleq \{ \boldsymbol{p} \in \Gamma : F_{i}(\boldsymbol{p}) = 0 \}$$

$$= \{ \boldsymbol{p} : i = 0 \} \cup \left\{ \boldsymbol{p} : i = 1 - \frac{\alpha}{\beta(1 - x)} \right\}$$
(13)

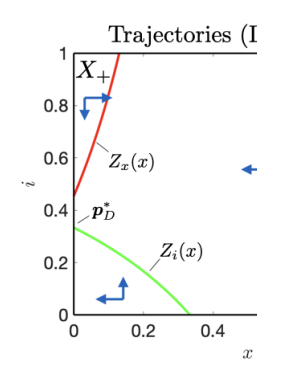
Note that p_D^* lies in the first component above. The x-isocline is

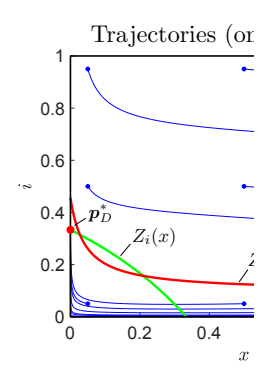
$$I_{x} \triangleq \{ \boldsymbol{p} \in \Gamma : F_{x}(\boldsymbol{p}) = 0 \}$$

$$= \{ \boldsymbol{p} : x = 0 \text{ or } 1 \} \cup \left\{ \boldsymbol{p} : i = \frac{x \delta_{TR1} + (1 - x) \delta_{PS1}}{x (\delta_{RT0} + \delta_{TR1}) + (1 - x) (\delta_{SP0} + \delta_{PS1}) \right\}$$
(14)

The intersection points of I_i and I_x in the state space Γ yield equilibrium points of the system. We call an equilibrium interior if it lies in Γ^0 . Observe that an interior equilibrium

 $^{^2 {\}rm Future}$ work will be devoted to establishing GAS of ${\boldsymbol p}_D^*$ in the omitted region.





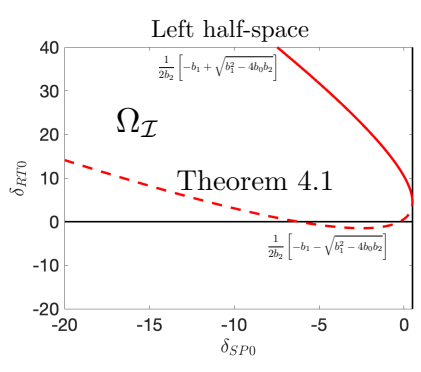


Fig. 1: (Left) The state space Γ and isoclines Z_x and Z_i in the regime of Lemma 4.1, $\delta_{SP0} < \delta_{SP0}^*$ and $\delta_{RT0} < 0$. Here, $\delta_{SP0} = 0.3$, $\delta_{SP0}^* = 0.5$, and $\delta_{RT0} = -2$. (Center) State trajectories (blue curves) in the parameter region omitted in Theorem 4.2. The blue circles indicate initial conditions. In this regime, two interior equilibria emerge from the intersection of Z_x and Z_i . The equilibrium p_D^* appears to be globally asymptotically stable. (Right) The left half-space with respect to payoff parameters ($\delta_{SP0}, \delta_{RT0}$). Lemmas 4.1 and 4.3 establish global asymptotic stability of p_D^* in the regions shown. The region omitted in Theorem 4.2 is the region above the solid red line. In all plots, we set $\delta_{TR1} = 1.5$, $\delta_{PS1} = 0.25$, $\alpha = 0.2$, and $\beta = 0.3$.

results from the intersection of the two curves

$$Z_{i}(x) \triangleq 1 - \frac{\alpha}{\beta(1-x)}$$

$$Z_{x}(x) \triangleq \frac{x\delta_{TR1} + (1-x)\delta_{PS1}}{x(\delta_{RT0} + \delta_{TR1}) + (1-x)(\delta_{SP0} + \delta_{PS1})}$$
(15)

More specifically, $(x, Z_i(x))$ is an interior equilibrium if and only if $Z_i(x) = Z_x(x)$ and $x \in (0, 1 - \frac{\alpha}{\beta})$. Detailed properties of the function Z_x are given in Appendix A. We begin the analysis by considering the lower-left quadrant.

Lemma 4.1. If $\delta_{SP0} < \delta_{SP0}^*$ and $\delta_{RT0} < 0$, then \boldsymbol{p}_D^* is GAS.

Proof. We first claim that there are no interior equilibria in this regime. A proof of this claim is provided in Lemma A.1 in the Appendix.

There are a total of three isolated equilibrium points: (0,0), p_D^* , and (0,1). We have shown that p_D^* is locally stable if $\delta_{SP0} < \delta_{SP0}^*$, and the other two rest points are unstable. To prove global asymptotic stability, we need to show there cannot be any periodic orbits in the interior Γ^o . The global stability then follows from the Poincaré-Bendixson Theorem. First, we consider the region $0 < \delta_{SP0} < \delta_{SP0}^*$. Here, $Z_x(x)$ intersects the state space Γ but does not intersect the i-isocline – see Figure 1 (Left). We can identify a non-empty subset

$$X_{+} = \{(x, i) \in \Gamma : i > Z_{x}(x)\} \subset \Gamma \tag{16}$$

for which $F_x(x,i)>0$ if $(x,i)\in X_+$ and $F_x(x,i)<0$ if $(x,i)\in\Gamma\backslash\bar{X}_+$. Here, \bar{X}_+ indicates the closure. We claim any trajectory that starts in X_+ leaves X_+ in finite time. To see this, observe the compact set \bar{X}_+ lies above (w.r.t. the i coordinate) and does not intersect the i-isocline. Hence, $F_i(x,i)< m_1<0$ for all $(x,i)\in\bar{X}_+$, where

$$m_1 = \max_{(x,i)\in \bar{X}_+} F_i(x,i).$$
 (17)

Hence, there cannot be any periodic orbit contained in \bar{X}_+ . We also have $F_x(x,i) < 0$ for all $(x,i) \in \Gamma \backslash \bar{X}_+$. Hence, there cannot be a periodic orbit contained in $\Gamma \backslash \bar{X}_+$.

Next, we claim any trajectory starting in $\Gamma \backslash \bar{X}_+$ can never enter \bar{X}_+ , i.e. $\Gamma \backslash \bar{X}_+$ is a positively invariant set that contains p_D^* . This fact follows from an application of Nagumo's Invariance Theorem. Let $h(x,i) = Z_x(x) - i$ defined for $(x,i) \in \Gamma$, such that $h(x,i) > 0 \to (x,i) \in \Gamma \backslash \bar{X}_+$. The boundary h(x,i) = 0 is precisely the x-isocline in Γ , and for any (x,i) satisfying h(x,i) = 0, $\dot{h}(x,i) = [F_x(x,i),F_i(x,i)] \cdot [\frac{\partial Z_x}{\partial x},-1] = [0,F_i(x,i)] \cdot [\frac{\partial Z_x}{\partial x},-1] > 0$. Since any trajectory starting in X+ ends up in $\Gamma \backslash \bar{X}_+$, and

Since any trajectory starting in \bar{X}_+ ends up in $\Gamma \backslash \bar{X}_+$, and $\Gamma \backslash \bar{X}_+$ is positively invariant with no periodic orbits (since $F_x(x,i) < 0$), we can conclude that there is no periodic orbit in Γ . By Poincaré-Bendixson, p_D^* is globally asymptotically stable.

Now, we consider the remaining region $\delta_{SP0} < 0$. The non-existence of periodic orbits here follows from the fact that $F_x(x,i) < 0$ for all $(x,i) \in \Gamma^o$. To see this, we consider the four possible cases from the proof of Lemma A.1.

• $Z_x(0), Z_x(1) < 0$. Then $Z_x(x) < 0$ for all $x \in [0,1]$. Note the numerator of Z_x , num(x), is positive for all $x \in [0,1]$. Hence, the denominator, $\operatorname{den}(x)$, must be negative for all $x \in [0,1]$. The condition that $F_x(x,i) < 0$ for any $(x,i) \in \Gamma^o$ is equivalent to

$$u_{\mathcal{C}}(x, 1-i) - u_{\mathcal{D}}(x, 1-i) = i \cdot \operatorname{den}(x) - \operatorname{num}(x) < 0$$

$$\iff i > Z_x(x)$$
(18)

which is satisfied.

- $Z_x(0), Z_x(1) > 1$. The fact that $F_x(x,i) < 0$ for all $(x,i) \in \Gamma^o$ follows analogous arguments from above.
- $Z_x(0) < 0$, $Z_x(1) > 1$. Here, $\operatorname{den}(x) < 0$ for $x \in [0, x_d)$ and $\operatorname{den}(x) > 1$ for $x \in (x_d, 1]$. For $x \in [0, x_d)$, the condition is equivalent to (18), which is satisfied here. For $x \in (x_d, 1]$, the condition is equivalent to $i < Z_x(x)$, which is satisfied here.
- $Z_x(0) > 1$, $Z_x(1) < 0$. The fact that $F_x(x,i) < 0$ for all $(x,i) \in \Gamma^o$ follows analogous arguments from above.

We now turn our attention to the remaining quadrant $\delta_{RT0} \geq 0$. Recall that solutions $x \in (0, 1 - \frac{\alpha}{\beta})$ to the equation

 $Z_i(x) = Z_x(x)$ yield interior equilibria. We find there can be at most two, which are found to be:

$$x_{\pm} \triangleq \frac{1}{2a_2} \left[-a_1 \pm \sqrt{a_1^2 - 4a_2 a_0} \right]$$
 (IPs)

where

$$a_{2} \triangleq \delta_{SP0} - \delta_{RT0}$$

$$a_{1} \triangleq \delta_{RT0} - 2\delta_{SP0} + \frac{\alpha}{\beta} \left(\delta_{SP0} + \delta_{PS1} - \delta_{RT0} - \delta_{TR1} \right)$$

$$= -(a_{0} + a_{2} + \frac{\alpha}{\beta} (\delta_{RT0} + \delta_{TR1}))$$

$$a_{0} \triangleq \left(1 - \frac{\alpha}{\beta} \right) \left(\delta_{SP0} - \delta_{SP0}^{*} \right)$$
(19)

Observe that x_{\pm} have non-zero imaginary part if and only if $a_1^2-4a_2a_0<0$. The following Lemma provides an equivalent condition in terms of the payoff parameters.

Lemma 4.2. Suppose $\delta_{SP0} < \delta_{SP0}^*$ and $\delta_{RT0} > 0$. The roots x_{\pm} from (IPs) have non-zero imaginary part if and only if

$$\frac{-b_1 - \sqrt{b_1^2 - 4b_0b_2}}{2b_2} < \delta_{RT0} < \frac{-b_1 + \sqrt{b_1^2 - 4b_0b_2}}{2b_2}$$
 (20)

where b_0 , b_1 , and b_2 are defined by (12).

Proof. The result follows by expressing $a_1^2 - 4a_2a_0 < 0$ using expressions from (19). We omit detailed calculations for brevity.

Let us denote $\Omega_{\mathcal{I}} \subset \mathbb{R}^2$ as the pairs of parameters $(\delta_{SP0}, \delta_{RT0})$ that satisfy (20). Because the roots are imaginary, the isoclines never intersect and hence there are no rest points in the interior. We can establish global asymptotic stability of \boldsymbol{p}_D^* in this regime. Note that the two bounds given in (20) coincide at $\delta_{SP0} = \delta_{SP0}^*$, yielding the value $\frac{\delta_{SP0}^* + \frac{\alpha}{\beta}\delta_{TR1}}{1 - \frac{\alpha}{\beta}}$.

Lemma 4.3. Suppose $\delta_{SP0} < \delta_{SP0}^*$ and $\delta_{RT0} > 0$. Then if $(\delta_{SP0}, \delta_{RT0}) \in \Omega_{\mathcal{I}}$ or $\delta_{RT0} \leq \frac{1}{2b_2} [-b_1 - \sqrt{b_1^2 - 4b_0b_2}]$, then \boldsymbol{p}_D^* is GAS.

Proof. Under the given conditions, one can show in a similar manner to Lemma A.1 that there are no interior equilibrium points. The proof of stability then follows similar arguments from Lemma 4.1 that were used for the first region $0 < \delta_{SP0} < \delta_{SP0}^*$. Essentially, one can identify a nonempty subset $X_+ \subset \Gamma$ and show that no periodic orbit can exist in Γ^o . We omit exact details for brevity.

The above result combined with Lemma 4.1 establishes Theorem 4.2.

V. NUMERICAL STUDIES: ENDEMIC EQUILIBRIUM WITH PARTIAL COOPERATION

In this section, we will consider the right half-plane $\delta_{SP0} \geq \delta_{SP0}^*$, in which p_D^* is no longer stable. We primarily study, through numerical simulations, stability properties of an *interior* endemic equilibrium that emerges in this regime. First, we establish a characterization of this equilibrium.

Proposition 5.1. Suppose $\delta_{SP0} > \delta_{SP0}^*$ and assume that $\delta_{TR1} - \delta_{PS1} > 0$. Then there is a unique interior equilibrium point, given by $\mathbf{p}_{int}^* \triangleq (x_-, Z_i(x_-))$, where x_- is given in (IPs).

Proof. The proof is omitted for space concerns.

The interior equilibrium $p_{\rm int}^*$ reflects an endemic epidemic state where a fraction of the population complies with health measures. The endemic level here is less severe than the level in p_D^* with full defection, where the infected fraction is $1-\frac{\alpha}{\beta}$. Simulating the dynamics, we observe a variety of dynamical outcomes and stability properties of the equilibrium $p_{\rm int}^*$. Sample trajectories are shown in Figure 2. These outcomes are linked to the eigenvalues of the Jacobian matrix $J(p_{\rm int}^*)$. In particular, Figure 2 (Left) indicates that

- In H_1 , the eigenvalues of $J(p_{\text{int}}^*)$ are real and negative. Here, we observe that p_{int}^* is GAS.
- In H_2 , the eigenvalues of $J(p_{\text{int}}^*)$ are a complex conjugate pair with negative real part. Here, we observe that p_{int}^* is GAS.
- In H_3 , the eigenvalues of $J(p_{\rm int}^*)$ are a complex conjugate pair with positive real part. Here, $p_{\rm int}^*$ is unstable and we observe trajectories converging to a stable limit cycle that contains $p_{\rm int}^*$.

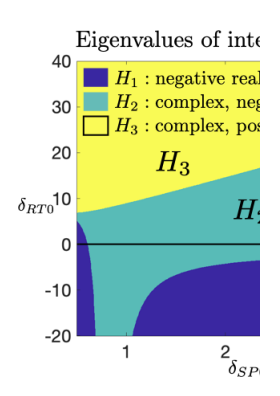
Thus, if we take δ_{RT0} as a bifurcation parameter, the stability properties of $\boldsymbol{p}_{\text{int}}^*$ change as it traverses up from H_1 to H_2 , and from H_2 to H_3 . From the numerical simulations, $\boldsymbol{p}_{\text{int}}^*$ undergoes a supercritical Hopf bifurcation as it traverses from H_2 to H_3 .

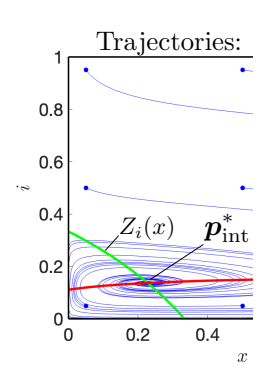
VI. CONCLUSIONS

We considered SIS disease dynamics coupled with population behavior. The population behavior modulated the change in the number of infected by adjusting the public's cooperation level with the recommended public health measures. The public's cooperation level evolves according to the replicator dynamics on game payoffs determined by the disease prevalence. We established the GAS of the endemic disease state with complete defection of public health measures based on the relative payoff values of the games in the good and bad states. Our results also show that the rich set of dynamics, e.g., stable limit cycles, bifurcations, exhibited as a result of the coupling between SEIR or SEIRS disease dynamics and population behavior [13] are retained when we consider the simpler SIS disease dynamics. The rich set of dynamics that arise as a result of the coupling between the game-theoretic behavior model and the disease dynamics, and the tangible set of payoff parameters related to the cost and benefits of public health measures provide suitable modeling framework for forecasting epidemics using available data.

REFERENCES

 S. Funk, M. Salathé, and V. A. Jansen, "Modelling the influence of human behaviour on the spread of infectious diseases: a review," *Journal of the Royal Society Interface*, vol. 7, no. 50, pp. 1247–1256, 2010.





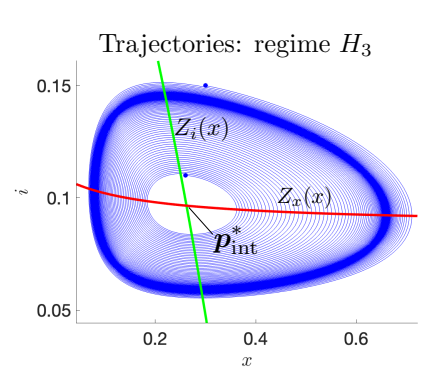


Fig. 2: (Left) Numerical characterization of the eigenvalues of the Jacobian at the unique interior equilibrium p^* in the right half-plane, $\delta_{SP0} \geq \delta_{SP0}^*$. (Center) State trajectories (blue curves) in the H_2 regime, where p^* has complex conjugate eigenvalues with negative real part. The initial conditions are shown as blue circles. p^* appears to be globally asymptotically stable. Here, $(\delta_{SP0}, \delta_{RT0}) = (2, 8)$. (Right) State trajectories from two initial conditions (blue dots) in the H_3 regime, where p^* has complex conjugate eigenvalues with positive real part. Trajectories appear to converge to a stable limit cycle that contains p^* . Here, $(\delta_{SP0}, \delta_{RT0}) = (2, 15)$. In all plots, we set $\delta_{TR1} = 1.5$, $\delta_{PS1} = 0.25$, $\alpha = 0.2$, and $\beta = 0.3$.

- [2] W. Abbas, M. MA, A. Park, S. Parveen, and S. Kim, "Evolution and consequences of individual responses during the covid-19 outbreak," Plos one, vol. 17, no. 9, p. e0273964, 2022.
- J. S. Weitz, S. W. Park, C. Eksin, and J. Dushoff, "Awareness-driven behavior changes can shift the shape of epidemics away from peaks and towards plateaus, shoulders, and oscillations.'
- [4] N. Perra, "Non-pharmaceutical interventions during the covid-19 pandemic: A review," Physics Reports, vol. 913, pp. 1-52, 2021.
- [5] M. Ye, L. Zino, A. Rizzo, and M. Cao, "Game-theoretic modeling of collective decision making during epidemics," Physical Review E, vol. 104, no. 2, p. 024314, 2021.
- [6] B. She, J. Liu, S. Sundaram, and P. E. Paré, "On a networked sis epidemic model with cooperative and antagonistic opinion dynamics," IEEE Transactions on Control of Network Systems, vol. 9, no. 3, pp. 1154-1165, 2022.
- [7] P. E. Paré, J. Liu, C. L. Beck, A. Nedić, and T. Başar, "Multicompetitive viruses over time-varying networks with mutations and human awareness," Automatica, vol. 123, p. 109330, 2021.
- [8] S. Funk, E. Gilad, C. Watkins, and V. A. Jansen, "The spread of awareness and its impact on epidemic outbreaks," Proceedings of the National Academy of Sciences, vol. 106, no. 16, pp. 6872–6877, 2009.
- [9] C. Eksin, K. Paarporn, and J. S. Weitz, "Systematic biases in disease forecasting-the role of behavior change," Epidemics, vol. 27, pp. 96-105, 2019.
- [10] W. A. Chiu, R. Fischer, and M. L. Ndeffo-Mbah, "State-level needs for social distancing and contact tracing to contain covid-19 in the united states," Nature Human Behaviour, vol. 4, no. 10, pp. 1080-1090, 2020.
- [11] C. Eksin, J. S. Shamma, and J. S. Weitz, "Disease dynamics in a stochastic network game: a little empathy goes a long way in averting outbreaks," Scientific reports, vol. 7, no. 1, pp. 1-13, 2017.
- A. Glaubitz and F. Fu, "Oscillatory dynamics in the dilemma of social distancing," Proceedings of the Royal Society A, vol. 476, no. 2243, p. 20200686, 2020.
- [13] H. Khazaei, K. Paarporn, A. Garcia, and C. Eksin, "Disease spread coupled with evolutionary social distancing dynamics can lead to growing oscillations," in 2021 60th IEEE Conference on Decision and Control (CDC). IEEE, 2021, pp. 4280-4286.
- [14] E. Elokda, S. Bolognani, and A. R. Hota, "A dynamic population model of strategic interaction and migration under epidemic risk," in 2021 60th IEEE Conference on Decision and Control (CDC). IEEE, 2021, pp. 2085-2091.
- [15] P. Poletti, M. Ajelli, and S. Merler, "The effect of risk perception on the 2009 h1n1 pandemic influenza dynamics," PloS one, vol. 6, no. 2, p. e16460, 2011.
- [16] A. Satapathi, N. K. Dhar, A. R. Hota, and V. Srivastava, "Epidemic propagation under evolutionary behavioral dynamics: Stability and bifurcation analysis," in 2022 American Control Conference (ACC). IEEE, 2022, pp. 3662-3667.
- [17] K. Frieswijk, L. Zino, M. Ye, A. Rizzo, and M. Cao, "A meanfield analysis of a network behavioral-epidemic model," IEEE Control Systems Letters, vol. 6, pp. 2533-2538, 2022.

- [18] J. S. Weitz, C. Eksin, K. Paarporn, S. P. Brown, and W. C. Ratcliff, "An oscillating tragedy of the commons in replicator dynamics with game-environment feedback," Proceedings of the National Academy of Sciences, vol. 113, no. 47, pp. E7518-E7525, 2016.
- [19] W. H. Sandholm, Population games and evolutionary dynamics. MIT Press, 2010.

APPENDIX

A. Properties of the x-isocline

The function $Z_x(x): \mathbb{R} \to \mathbb{R}$ possesses the following properties. It has a single point of discontinuity at

$$x_d \triangleq \frac{-(\delta_{SP0} + \delta_{PS1})}{\delta_{RT0} + \delta_{TR1} - (\delta_{SP0} + \delta_{PS1})}.$$
 (21)

Thus, $Z_x(x)$ is defined for all $x \in \mathbb{R} \setminus \{x_d\}$. Z_x is strictly monotone on $\mathbb{R}\setminus\{x_d\}$.

- If $\delta_{SP0}\delta_{TR1} \delta_{PS1}\delta_{RT0} > 0$, then $Z_x(x)$ is strictly increasing on $\mathbb{R}\setminus\{x_d\}$. It holds that $Z_x(x)$ strictly increasing on Taylor (wa). It notes that $Z_x(x) > \frac{\delta_{TR1} - \delta_{PS1}}{\delta_{TR1} - \delta_{PS1} + \delta_{RT0} - \delta_{SP0}}$ for $x < x_d$ and $Z_x(x) < \frac{\delta_{TR1} - \delta_{PS1}}{\delta_{TR1} - \delta_{PS1} + \delta_{RT0} - \delta_{SP0}}$ for $x > x_d$.

 • If $\delta_{SP0}\delta_{TR1} - \delta_{PS1}\delta_{RT0} < 0$, then $Z_x(x)$ is
- strictly decreasing on $\mathbb{R}\setminus\{x_d\}$. It holds that $Z_x(x)$ stitity decreasing on $\mathbb{E}(\{u_a\}, R)$ holds that $Z_x(x) > \frac{\delta_{TR1} - \delta_{PS1}}{\delta_{TR1} - \delta_{PS1} + \delta_{RT0} - \delta_{SP0}}$ for $x < x_d$ and $Z_x(x) > \frac{\delta_{TR1} - \delta_{PS1} + \delta_{RT0} - \delta_{SP0}}{\delta_{TR1} - \delta_{PS1} + \delta_{RT0} - \delta_{SP0}}$ for $x > x_d$.

 • If $\delta_{SP0}\delta_{TR1} - \delta_{PS1}\delta_{RT0} = 0$, then it takes the constant value $Z_x(x) = \frac{\delta_{PS1}}{\delta_{SP0} + \delta_{PS1}}$ for all $x \in \mathbb{R}$.

Lemma A.1. If $\delta_{SP0} < \delta_{SP0}^*$ and $\delta_{RT0} < 0$, then there are no rest points in Γ^0 .

Proof. The proof is omitted for space considerations.